



Ben-Gurion University of the Negev  
Faculty of Engineering Science

School of Electrical and Computer Engineering  
Dept. of Electrical and Computer Engineering

Fourth Year Engineering Project  
Final Report

Experimental setup for NOEMS

<b>Project number:</b>	<b>p-2024-051</b>
<b>Students:</b>	Yaakov Kuzminsky 206511966 Oren Sberro 208118562
<b>Supervisors:</b>	Prof. Karabchevsky Alina Maya Shor Peled
<b>Submitting date:</b>	18/08/2024

## **Table of contents:**

Abstract.....	3
The objective of the Project.....	4
Introduction.....	4
Schematic of the system.....	7
Design approach & solution.....	9
Results & Verifications.....	12
Problems & solutions.....	14
Conclusions & Recommendations.....	17
References.....	19
Appendices.....	20

## **1. Abstract**

### **Experimental setup for NOEMS**

Student's name: Kuzminsky Yaakov, Sberro Oren

*e-mail: kuzminsk@post.bgu.ac.il*

Adviser's name: Prof. Alina Karabchevsky, Maya Shor Peled

### **1.1 English Abstract**

Understanding biological systems at the nanoscale is crucial for insights into disease mechanisms and cellular processes, necessitating advanced imaging techniques beyond the diffraction limit of conventional microscopy. To address this challenge, this project aims to enhance an existing experimental setup for super-resolution imaging using photonic nano-jets (PNJ) and photonic hooks (PH). The objectives include achieving higher resolution and stability in imaging, as well as recreating and studying PNJ and PH phenomena. We propose an optimized setup combining an LED and a laser to generate and observe PNJ and PH with greater precision. The method involves designing and simulating an optical setup using a microcylinder and mask to generate PNJ and PH, aligning components on three-axis stages, and validating through experimental results and comparisons to literature setups. Expected results include higher stability and resolution in imaging, and successful recreation and observation of PNJ and PH phenomena.

**Keywords:** Super-resolution imaging, photonic nano-jet, photonic hook, microcylinder.

### **1.2 Hebrew Abstract**

הבנת מערכות ביולוגיות בסקלה ננומטרית הינה הכרחית כדי לקבל תובנות במנגנוני מחלה ותהליכים תאיים, מה שמחייב טכניקות הדמאה מתקדמות, המתאפשרות הדמאה למעבר לגבול הדיפרקציה של מיקרוסקופיה קונבנציונלית. כדי להתמודד עם אתגר זה, הפרויקט זה שואף לשפר מערך ניסוי קיים לסופר-רזולוציה, ע"י שימוש בPNJ ו PH. השיפור כולל הגעה לרזולוציית הדמאה גבוהה יותר, הדמאה יציבה יותר והצלחה של שחזור תופעת ה PH ולמידתה באמצעות מערך הניסוי בלבד. אנו מציעים מערך ניסוי חדיש, בו ע"י שילוב של מקורות אור של לד ולייזר, ניצור ונצפה בתופעות הפיזיקליות הנ"ל. שיטת העבודה תהיה בעזרת סימולציות של מערך הניסוי, הצילינדר והמסכה לייצור הPNJ וה PH. לאחר מכן, ייצוב והתאמה של כל הרכיבים פיזית במערכת הניסוי ע"י שימוש בבמות מכוננות ב-3 צירים. לבסוף, אישוש התוצאות ע"י השוואה לסימולציות ולתוצאות עבר. הצלחת הפרויקט תימדד בהשגת רזולוציית הדמאה גבוהה יותר, יציבות גבוהה יותר בהדמאה ויצור וצפייה מוצלחת בתופעות הפיזיקליות. **מילות מפתח:** הדמאה בסופר רזולוציה, פוטוניק ננו-ג'ט, פוטוניק הוק, מיקרוצילינדר.

## **2. The Objective of the Project**

The objective of this project is to enhance an existing experimental setup designed for super-resolution imaging of nanoscale objects using the photonic nano-jet. The upgraded setup aims to achieve higher resolution and improved stability. In addition, the setup aims to recreate the Photonic nano-jet (PNJ) and Photonic hook (PH) phenomena, study and characterize it. If succeeded, it will enable imaging of nanoparticles not only utilizing the PNJ but also the PH.

## **3. Introduction**

Understanding biological systems, such as disease origins and prognoses, relies heavily on insights gained at the single-cell level—a critical field in molecular biology and medicine. Additionally, due to the complexity and high organization of biological systems, advanced photonic tools hold the potential to allow researchers and clinicians to visualize, track, control, and manipulate biological processes at the single-cell level, both spatially and temporally. The most common method for observing samples involves magnifying them with a lens using visible light. However, the wave nature of light imposes a limit on resolution in optical microscopy, known as the diffraction limit, as initially described by Ernst Abbe [1]. This limit dictates the maximum resolution achievable by a conventional optical microscope in distinguishing between objects, expressed as

$$(1) \quad d = \frac{k\lambda}{2NA}$$

As  $d$  is the distance between two-point sources,  $\lambda$  stands for the wavelength and  $NA$  is the numerical aperture. when the coefficient  $k$  is typically within the range of 0.473-0.61 leading to the resolution to be within the range of 200-500 nm. Despite these theoretical predictions, practical implementation faces challenges, due to inherent aberrations and imperfections in classical optics. Thus, while theoretical calculations provide promising resolution estimates, practical limitations hinder the realization of optimal imaging capabilities in optical microscopy. Optical tweezers, pioneered by Arthur Ashkin, stand as a scientific instrument engineered for the manipulation of small objects, such as cells or molecules [1]. Ashkin's groundbreaking contributions in this field culminated in his receipt of the Nobel Prize in 2018. Central to the operation of optical tweezers are directed and focused laser beams, which allow precision in

controlling the positioning and mobility of objects within intricate cellular environments, achieving this by manipulating the particles using radiation pressure and the Lorentz force [1]. However, employing optical tweezers for microparticle manipulation encounters obstacles such as imprecise manipulation due to a bulky lens system and limited penetration depth. With biomolecules typically around 110 nm in diameter, direct manipulation using optical tweezers faces obstacles due to the diffraction limit of light.

There are methods to surpass Abbe's diffraction limit, yet many face significant challenges. Some are inherently irreversible and destructive, leading to permanent alterations in proteins or molecules upon application [1]. To overcome the complexities described above, we must surpass Abbe's diffraction limit without harming the objects we aim to study. This is known as Super-resolution imaging, encompassing a range of far-field optical microscopies capable of producing images with resolutions beyond the diffraction limit of light. One such technique employing super-resolution is the utilization of Photonic Nano-jet (PNJ).

A PNJ is a narrow light beam situated near the shadow-side surface of an illuminated dielectric microsphere, whose diameter is comparable with one or a few wavelengths of the light source [1]. There are few key characteristics of the PNJ: high intensity (up to  $\times 100$  of the incident power density), subdiffractional beam width and several wavelengths' long reach.

Several methods exist for generating Photonic Nano-jets (PNJ), and the method we employ involves the use of microcylinders [2]. Previous studies have demonstrated that PNJs can be produced using various combinations of refractive indices ( $n_2$  for the background and  $n_1$  for microcylinders), wavelength ( $\lambda$ ), and microcylinder diameter ( $D$ ). It has been shown that, provided the ratios of  $n_1/n_2$  and  $D/\lambda$  remain constant, the properties of the generated PNJ remain unchanged. However, increasing the microcylinder diameter causes the nanojet to move further away from the microcylinder, and its maximum intensity and full width at half maximum (FWHM) also increase [2].

When approaching Super-resolution for asymmetric particles, there is another phenomenon that can be implemented - curved photonic hook (PH), which merges the physical principles underlying photonic nano-jet (PNJ). This breaking of symmetry generates structured light beams that curve, forming what is known as a curved photonic jet or PH [1]. The photonic hook (PH) exhibits distinctive characteristics, including a tilt angle that varies with deformation. A study by Maya H.M.S. et al., titled "Ultrashort Pulsed Beam-Induced Nanoparticles Displacement

Trajectories via Optical Forces in Symmetrical and Symmetry-Breaking Systems" [3], has investigated the potential of employing PH for nanoparticle manipulation. If successfully harnessed, this could enhance the efficacy of optical tweezers, enabling non-symmetrical manipulation. The generation of PHs can be achieved through various techniques designed to break symmetry.

One approach involves employing a microcylinder composed of two different refractive indexes. [4]. Another approach is to utilize the focusing of a plane wave through an asymmetric dielectric particle, such as a combination of a wedge prism and a cuboid [5]. The method we are employing involves selectively blocking part of the input light using an auxiliary structure. This technique enables precise control over the resulting angle of the hook, defined by the tilt angle  $\theta$ , which can be adjusted by varying the thickness of the blocked beam, with the assistance of a mask under different heights ( $h$ ). Notably, the scenario with  $h = 0$  corresponds to the classical PNJ for a dielectric microcylinder. By selective blocking of part of the input light, we can manipulate the PH's shape and curvature radius. When changing the mask height from  $h=0$  to 0.5, we can observe the curvature changes of the PH [6].

The rationale behind selecting the last approach can be understood by examining the conclusions outlined in the article by Maya Hen Shor Peled et al. [3] The study investigates the motion of a particle manipulated by a Photonic Hook (PH) when the beam is obstructed by various plate heights. Three distinct types of motion were observed: negative direction motion, where the nanoparticle is attracted towards the cylinder; positive direction motion, where the nanoparticle is repulsed; and an oscillatory motion, where the nanoparticle is confined within a finite region (around or between stable points) [3]. It is evident from the study's conclusion that certain plate positions may lead to a higher probability of each type of motion. This insight could prove invaluable in designing experimental approaches for nanoparticle manipulation tailored to specific applications. For instance, when the plate is positioned at a quarter of the cylinder diameter, it results in the highest number of stable trajectories, where the nanoparticle oscillates around a stable point.

In comparison to the classical PNJ, the spatial resolution of the PH is relatively lower. However, the advantage of the PH lies not in its ultra-high spatial resolution, but rather in its ability to bend at subwavelength scales. It's important to note that increasing the curvature of the PH comes at the expense of reducing the maximum intensity of the focus. Despite the trade-off in spatial

resolution, photonic hooks hold tremendous potential in various applications such as super-resolution imaging, surface fabrication, and optomechanical manipulation along curved trajectories.

#### **4.Schematic of the system**

The design of the optical setup for our experiment is based on an extensive literature review, particularly following the guidelines outlined in "Experimental demonstration of a tunable photonic hook by a partially illuminated dielectric microcylinder." By Minin Igor et al. [6] and is illustrated in Figure 4.1. All components are mounted on three-directional movable stages- Thorlabs MBT616D, allowing precise alignment of the laser beam to target either the microcylinder or the mask. The experimental system includes a Qioptiq Photonics iFLEX-iRIS CLM solid-state laser with 100 mW output power and a Thorlabs RC04FC-P01 collimator. The laser beam travels through the collimator and then in open space, striking either the mask or the microcylinder, depending on whether we aim to observe the photonic hook (PH) or the photonic nanojet (PNJ). The mask -a fully reflective metal, is positioned such that moving its stage along the Y-axis can block or unblock the beam, introducing asymmetry in the system and creating the PH, while the microcylinder is secured and positioned beneath the imaging setup. The imaging system is based on the previous year's setup, as seen in Figure 4.2, with key modifications: the light source of the imaging setup has been switched to an LED -Thorlabs M505F3(505 nm, 8.5 mW) and an appropriate collimator (RC04FC-P01) to enhance image stability and facilitate the use of the laser for both PNJ and PH observations. The LED light passes through a 50/50 Beam Splitter (Thorlabs, CCM1-BS013), and the collected light is focused using a 100x magnification objective (Zeiss, LD EC Epiplan-Neoflaur, NA=0.75) to achieve high resolution. This light reaches the substrate where the microcylinder is located, reflects off it, and is directed to a Plano Convex Lens (Thorlabs, LA1484). Finally, the light is gathered onto a CCD camera (Thorlabs, CMOS camera DCC1645C 1280x1024) and transmitted to a computer for imaging. The constructed setup in the laboratory is shown in Figure 4.9, with Figures 4.3-4.8 illustrating all the components of the optical setup individually.

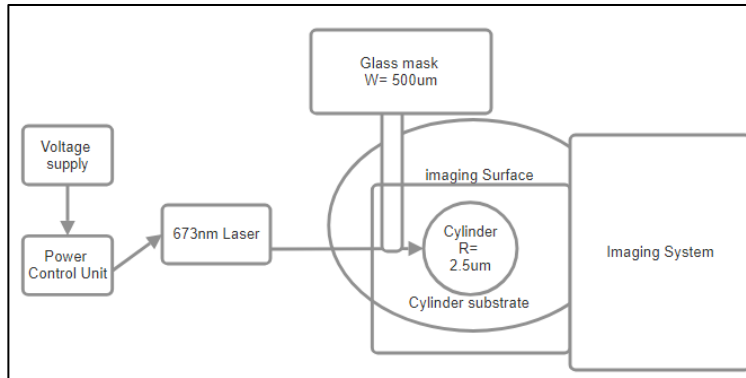


Figure 4.1: Schematic of the Setup



Figure 4.2: Last year's imaging setup

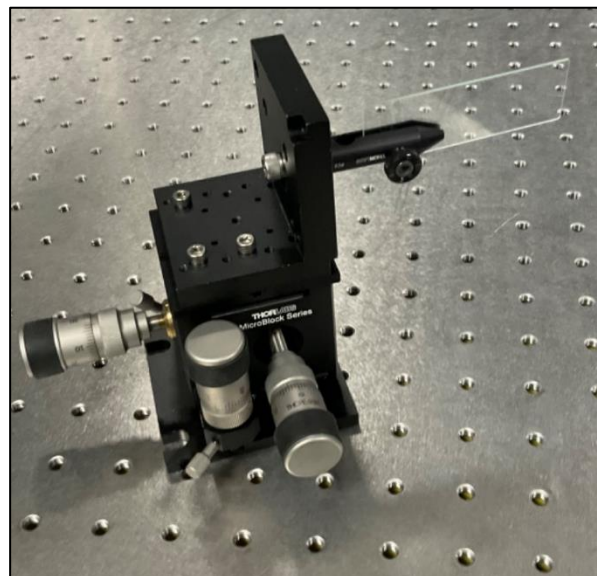


Figure 4.3: Movable stage with the mask





Figure 4.4: Movable stage with Laser

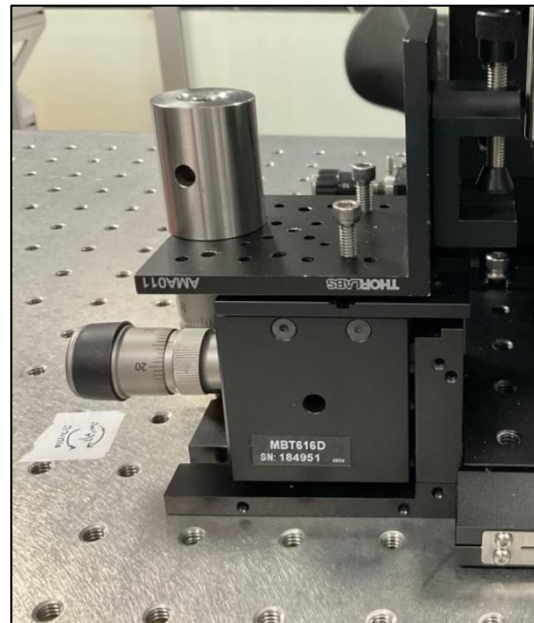


Figure 4.5: Movable stage with Catcher for the Microcylinder



Figure 4.6: Power Supply

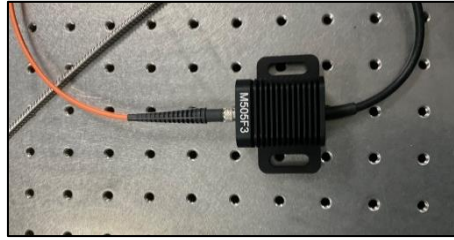


Figure 4.7: 505nm LED

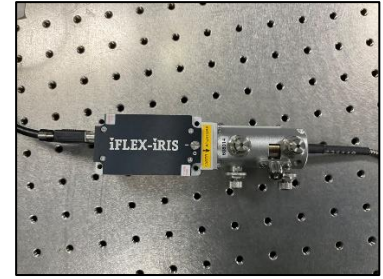


Figure 4.8: 673nm Laser

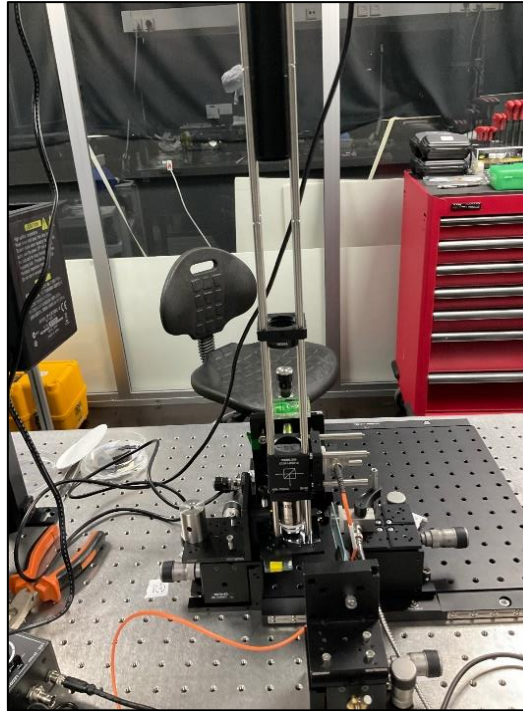


Figure 4.9: Full Experiment Setup

### **5.Design approach & solution:**

Our initial experiment setup was derived from last year's project [7] as illustrated in figure 4.2. We began by thoroughly understanding their setup, including its design, physical approach, and limitations. After reviewing relevant literature and analyzing their proposed setup, we gained the insights needed to improve and adapt their setup for a wider range of uses.

Before designing our new model, we wanted to simulate the PNJ and PH to gain a deeper understanding. We also needed to learn about the properties of key components, such as microcylinders, masks, and lasers. Using 'Lumerical' for computer simulations, we modeled the PNJ and PH phenomena by varying the properties of each component and analyzing the results, as shown in figures 6.3-6.5. These simulations enhanced our understanding and allowed us to evaluate whether the microcylinder produced for us in the lab was suitable for our needs.

In last year's setup, a 637nm laser was used to observe and create the PNJ phenomena via fiber optics. Based on the diffraction limit formula, we determined that a 505nm LED with a proper collimator could enhance the resolution we wanted to achieve. This LED could effectively replicate the observations made with the 637nm laser. In our experimental setup, we proposed an innovative solution for creating both PNJ and PH phenomena. We used the 505nm LED (figure 4.7) for observation and a 673nm laser (figure 4.8) with its own collimator as a side light source to generate the PNJ and PH phenomena. By combining these two light sources, we can achieve greater precision and resolution in observing the phenomena.

To accurately perform the phenomena, we knew that all components needed to be aligned at the same height thus recognizing the need for additional components. We determined that we required three stages capable of movement along all three axes with precise control at the micron level, as the phenomena involve small scales. We selected the 'Thorlabs MBT616D' 3-axis stage, which provides fine and coarse resolutions of 50 $\mu$ m and 500 $\mu$ m, respectively. We used this for the laser, the mask, and the microcylinder stages, while the LED and CCD camera utilized the optical stage from last year's setup, which has a resolution of 25 $\mu$ m.

Each component required adjustments to the stages due to their unique shapes to ensure they fit our configuration without disrupting the setup. For the laser stage, we added a "V"-shaped surface that can be placed on top and secured. For the mask stage, we used an additional tweezer mechanism (figure 4.3) to hold the mask, and for the microcylinder stage, we included a catcher (figure 4.5) designed to securely hold the cylinder in place. Each of these components can be precisely adjusted using the stage movements.

To create the PNJ phenomena, we used a microcylinder which was fabricated in a university lab with a radius of 3 $\mu$ m, a height of 11 $\mu$ m, and a refractive index of 1.63, which is placed above a bigger sample surface as determined from our simulations. To induce the PH phenomena

and break the symmetry, we used a glass plate with a width of  $500\mu\text{m}$ , which would partially block the laser beam as required.

Since the microcylinder could be damaged by overheating, we needed to carefully adjust the laser's output power. We reached out to suppliers at 'Qioptiq' to understand the properties of the laser and learned that its power could be adjusted by varying the input voltage. We used an additional power supply (figure 4.6) and determined that the required voltage range was between 0.3V and 0.6V. Additionally, we employed a collimator to narrow and better focus the laser beam, ensuring it was more coherent and suitable for our experiment. Figures 5.1 and 5.2 display



Figure 5.1: Laser output power



Figure 5.2: Open space Division

the laser output power and the open space division as measured with a power meter. Based on our calculations, this output power is sufficiently low to prevent damage to the cylinder.

When placing all the components, we had to consider the stability of the setup, as even minor movements or instabilities—sometimes imperceptible to the human eye—could have significant impacts. We also needed to ensure accessibility for manual operation and accommodate potential future automation. Proper distances between the laser, microcylinder, and mask were crucial. This setup relied on the special Thorlabs table in the lab, which has holes to facilitate these necessary adjustments. The result is shown in figure 4.9.

As we placed all the components in their designated positions, we needed to fully grasp the scale we were working with. Since the process was conducted manually, our spatial understanding was crucial. To assist with this, we requested that the sample surface be marked with a large arrow pointing towards the microcylinder. This prominent arrow made it easier to locate the microcylinder and provided a general measure of the spatial distance from the arrow to the main border, significantly enhancing our spatial orientation.

## **6.Results & Verifications**

Our first verification method for assessing our success was to compare our results with those from last year's project. One of our project goals was to stabilize the setup further and confirm our assumptions about the 505nm LED.

We used the same sample and fiber optics that last year's students used, which allowed for a direct comparison of results. We were pleased to find that our setup demonstrated improved stability and that our assumptions about the 505nm LED were accurate in practice, as illustrated in figures 6.1 and 6.2. Furthermore, we achieved more stable imaging of the grid and succeeded in imaging it without using the fiber optic setup to implement the PNJ for super-resolution. The color differences observed in the figures are due to the change in the wavelength of the light imaging source.

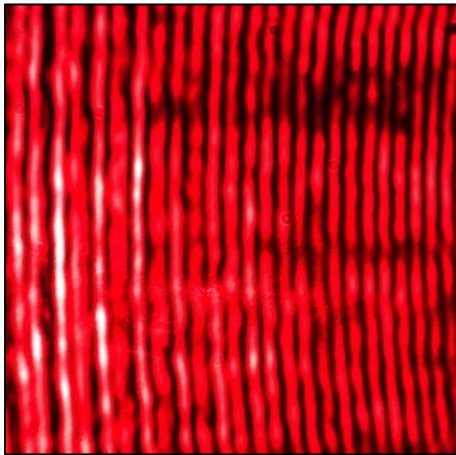


Figure 6.1: Last year's setup imaging of a grid with 0.8 $\mu$ m distance between lines.

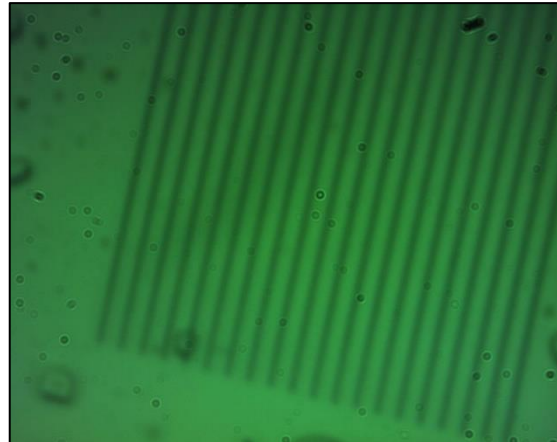


Figure 6.2: Our imaging of a grid with 0.8 $\mu$ m distance between lines.

Our main goal for the project was to recreate the PNJ and PH phenomena. We began by simulating these phenomena using 'Lumerical.' These simulations were crucial for understanding the phenomena. While we recognized that computer simulations can provide idealized results, they allowed us to compare and validate whether our project outcomes were consistent and made sense. For the simulations, we used a microcylinder with a 3  $\mu$ m radius cylinder, 10  $\mu$ m height, and



a refractive index of 1.63, a 673 nm laser, and a metal mask. We performed three simulations where the mask covered 0, 0.25, and 0.5 parts of the cylinder as shown in figure 6.3-6.5.

The results showed that we achieved an approximate 0.5-1 $\mu$ m PNJ and PH beam. Additionally, as the mask covered less of the cylinder, the electrical density was higher.

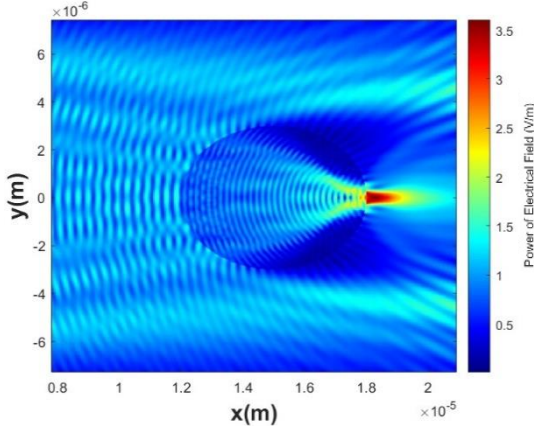


Figure 6.3: PNJ simulation

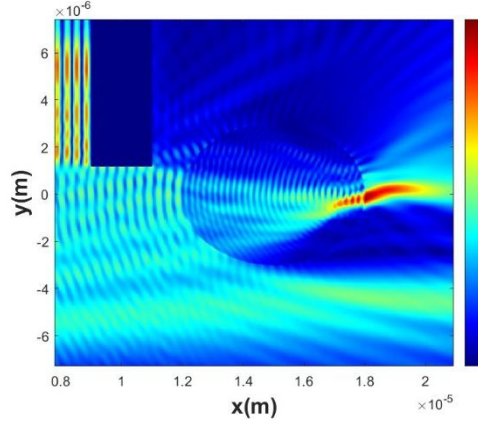


Figure 6.4: PH simulation,  $h=0.25$

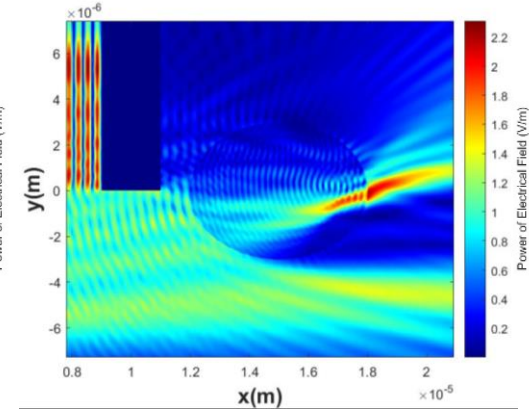


Figure 6.5: PH simulation,  $h=0.5$

After designing our setup and verifying its stability, we performed our experiment. We created the PNJ phenomena first as described in the literature and performed in the simulation, using a 3 $\mu$ m radius microcylinder. In Figure 6.6, we observed the entry of the laser beam hitting the microcylinder. Figure 6.7 shows the propagation of the laser beam through the cylinder, and Figure 6.8 illustrates the creation of the PNJ phenomena. Additional result images can be found in the appendix in Figures 10.1-10.6

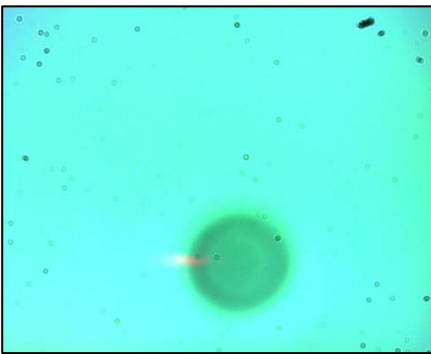


Figure 6.6: Laser entry

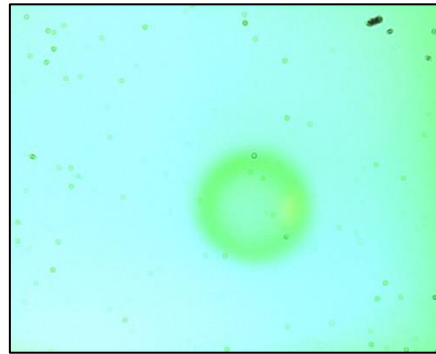


Figure 6.7: Laser propagation

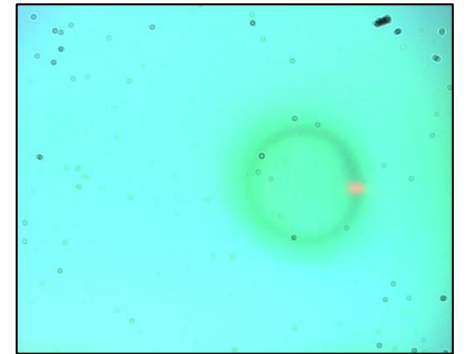


Figure 6.8: PNJ phenomena

Our second objective was to create the PH phenomena by breaking the laser beam symmetry using a mask. Figure 6.9 shows the results we obtained in the lab.

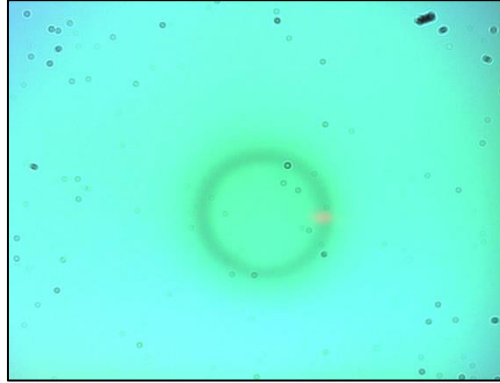


Figure 6.9: Laser propagation

### **7.Problems & solutions:**

During our project, we encountered several challenges related to working within the nanometer scale. The entire setup was controlled manually by us, which included moving the pulleys for the axles and adjusting the height of the CCD and LED stages. This manual control made it difficult to achieve precise micron-level accuracy. Additionally, maintaining orientation at the nanometer scale and locating our microcylinder proved challenging. The microcylinder itself was very fragile and, unfortunately, broke once during the process. However, this incident ultimately contributed to our understanding and improvements in the setup.

The first sample we received had a single large arrow outside the sample, far from the microcylinder, which did not provide much assistance. To address the orientation problem, after breaking the first cylinder, we designed a new sample with three microcylinders, with radius sized  $1.8\mu\text{m}$ ,  $2.4\mu\text{m}$ , and  $3\mu\text{m}$ , as seen in Figures 7.1-7.3.

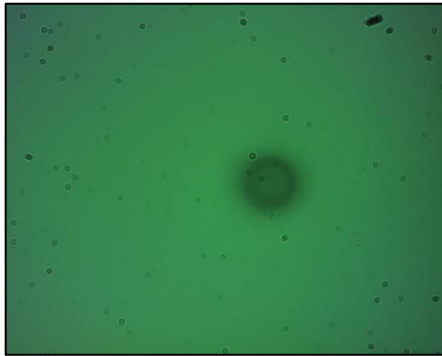


Figure 7.1: 1.8 $\mu\text{m}$  radius cylinder

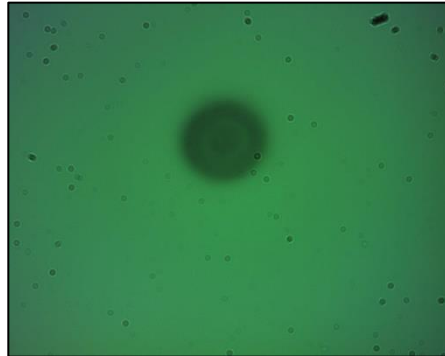


Figure 7.2: 2.4 $\mu\text{m}$  radius cylinder

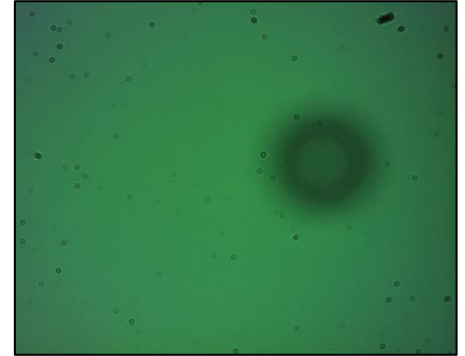


Figure 7.3: 3 $\mu\text{m}$  radius cylinder

Each microcylinder had a large arrow close to it inside the sample, as shown in Figure 7.4, pointing directly at it, which greatly aided in navigating and quickly locating the cylinders.

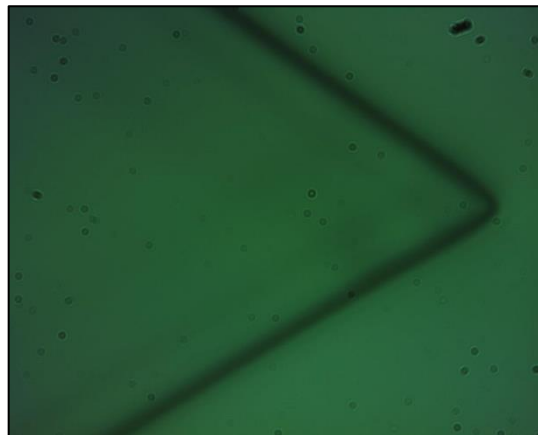


Figure 7.4: Arrow

As described above, a major issue we faced was that even the slightest movement or pressure could destabilize the setup and cause it to go out of focus. Ensuring complete stability and alignment at the nanometer scale proved to be quite challenging.

To address these issues, we initially used levelers to improve alignment accuracy. However, even the most precise levelers measure in millimeters, making them insufficient for our needs. Much of the alignment was therefore performed by eye, relying on trial and error to make the necessary small adjustments.



An additional challenge we faced while working on a small scale was understanding the scale of the objects we were observing through our system. Since we were looking for a cylinder with a radius of just a few microns, we needed to grasp the scale of what we were expecting to see. To address this, we used a grid sample from last year's students, which featured lines with a width of  $0.18\text{ }\mu\text{m}$  and varying distances between them. We designated the distance between lines as  $d$ . The distances for each row were as follows: first row  $d = 1.9\text{ }\mu\text{m}$ , second row  $d = 0.8\text{ }\mu\text{m}$ , third row  $d = 0.5\text{ }\mu\text{m}$ , fourth row ( $d = 0.3\text{ }\mu\text{m}$ , and fifth row  $d = 0.1\text{ }\mu\text{m}$ . This allowed us to achieve the scale understanding we needed. The grid's imaging through our system is shown in Figures 7.5-7.8.

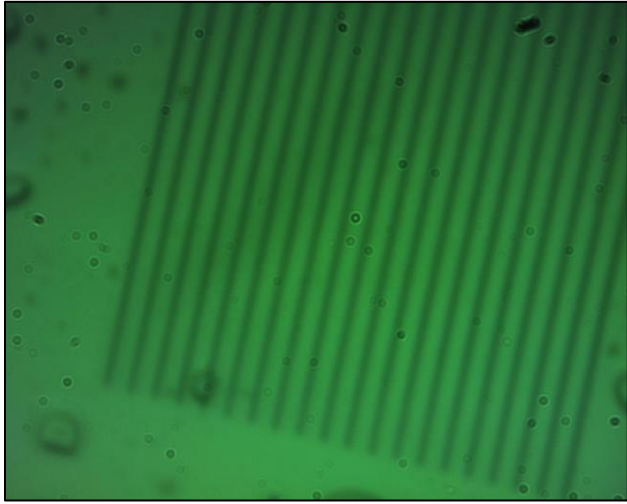


Figure 7.5: Second Row imaging ( $d=0.8\text{ }\mu\text{m}$ )

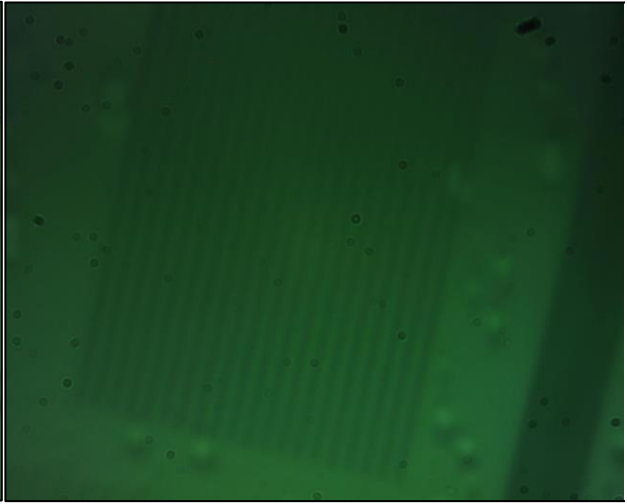


Figure 7.6: Third Row imaging ( $d=0.5\text{ }\mu\text{m}$ )

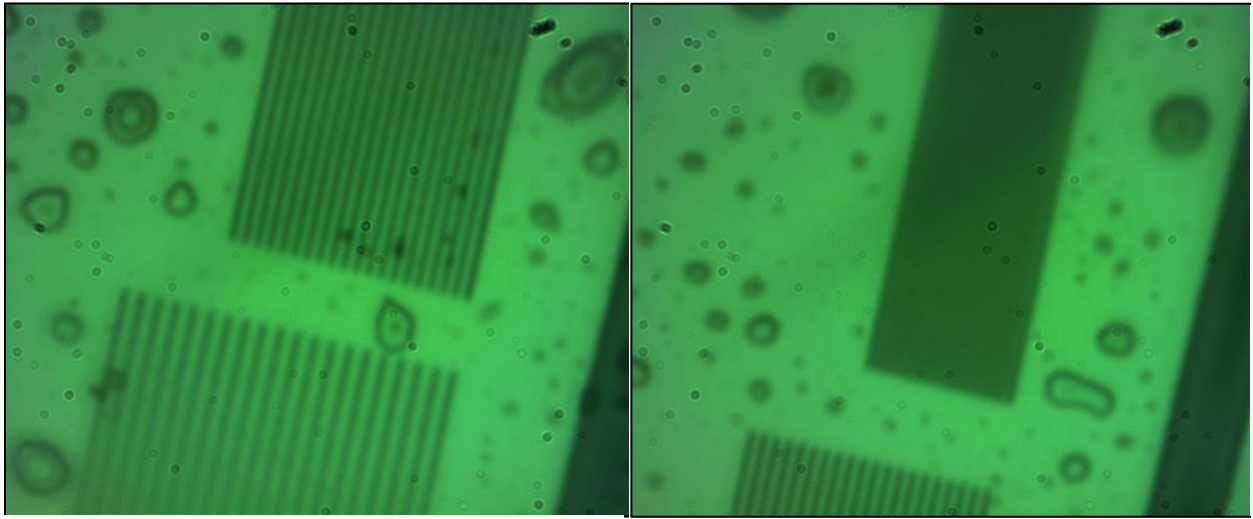


Figure 7.7: Third Row imaging ( $d=0.3 \mu\text{m}$ )

Figure 7.8: Fourth Row imaging ( $d=0.1 \mu\text{m}$ )

Another Problem that we had to address is that the microcylinder could overheat from the laser, which has the potential to cause damage. To resolve this, we measured the laser's output power using a power meter and found that it needed to be reduced and carefully controlled. We achieved this by connecting an external power supply to the laser, allowing us to manually adjust and control its output. The graph depicting the relationship between output power and control voltage is shown in Figure 7.9.

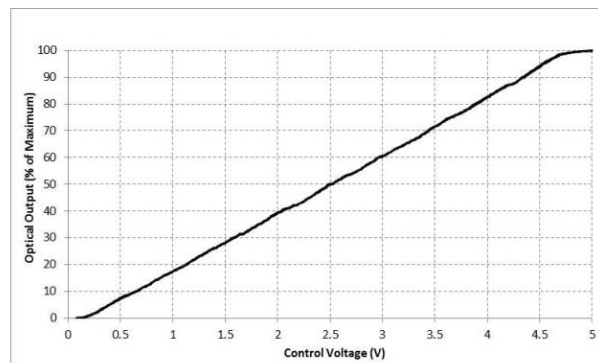


Figure 7.9: Laser output power in relation to control

## **8. Conclusions & Recommendations:**

First and foremost, we successfully designed and constructed an experimental setup that facilitates super-resolution imaging using PNJ and PH techniques. As previously discussed, our setup demonstrates enhanced stability and resolution, achieved by optimizing the light source in the imaging system. This advancement is evident in Figures 7.1-7.3, which display the second set of fabricated microcylinders with radii of  $2.4\mu\text{m}$ ,  $1.8\mu\text{m}$ , and  $3\mu\text{m}$ . Notably, the previous setup could only achieve imaging at these scales using PNJ, whereas our current setup achieves similar imaging capabilities using only the 505 nm LED.

Additionally, we have successfully recreated and observed the PNJ phenomenon, as can be seen in Figure 6.8, where the experiment was conducted on the largest cylinder with a radius of  $3\mu\text{m}$ . Figure 6.6 and 10.1-10.3 show the 673 nm laser light (depicted in red) entering the cylinder, while Figure 6.7 demonstrates the light's propagation through the cylinder, observable by adjusting the focus of the imaging setup. Finally, Figures 6.8 and 10.4-10.6 depict the beam exiting the cylinder. According to simulations, the exiting beam should be focused around the vertical center of the cylinder. Our results align with this prediction; however, we observed that the beam was significantly smaller than expected, measuring approximately  $0.5\mu\text{m}$  in length compared to the  $1\mu\text{m}$  predicted by simulations, as seen in Figures 6.3-6.5. This discrepancy is likely due to imperfections in cylinder fabrication, which cause the light to spread rather than focus. Additionally, issues with system alignment and insufficient laser power, which may not fully penetrate the cylinder or reach the objective, contribute to this outcome.

Regarding the PH phenomenon, we observed a reduced intensity of the exiting beam (Figure 6.9) and were unable to detect the anticipated curvature. We attribute this primarily to the insufficient resolution of the current setup. As shown in Figures 7.6-7.8 - we can resolve differences in objects down to approximately  $0.3\mu\text{m}$ , which makes it challenging to identify a beam of similar scale. To improve this, we recommend using a laser with a more focused beam, this would enhance precision and reduce the impact of reflections. Additionally, fabricating a wider cylinder may contribute to better results as discussed in the Introduction section.

Considering the challenges encountered, we propose that automating the setup is essential for improving our precision and efficiency. Implementing an automated system would eliminate

human error and provide precise control over the movements. Additionally, developing an application to integrate a sample scale and specify the movements of the camera and stages would significantly enhance accuracy and save time spent navigating space manually.

Another suggestion is to examine the sample under a high-quality microscope first to understand its scale and check for any damage or contaminants. This initial inspection would help ensure the sample's integrity before proceeding with more precise measurements and adjustments.

## **9.References:**

- [1] Karabchevsky, Alina, et al. "Super-Resolution Imaging and Optomechanical Manipulation Using Optical Nanojet for Nondestructive Single-Cell Research." *advanced photonics research* 3.2 (2022): 2100233.
- [2] Darafsheh, Arash. "Photonic nanojets and their applications." *Journal of Physics: Photonics* 3.2 (2021): 022001.
- [3] Peled, Maya Hen Shor, et al. "Ultrashort pulsed beam induced nanoparticles displacement trajectories via optical forces in symmetrical and symmetry-breaking systems." *Optics & Laser Technology* 168 (2024): 109937.
- [4]Gu, Guoqiang, et al. "Photonic hooks from Janus microcylinders." *Optics express* 27.26 (2019): 37771-37780.
- [5] Yue, Liyang, et al. "Photonic hook: a new curved light beam." *Optics letters* 43.4 (2018): 771-774.
- [6] Minin, Igor V., et al. "Experimental demonstration of a tunable photonic hook by a partially illuminated dielectric microcylinder." *Optics Letters* 45.17 (2020): 4899-4902.
- [7] Mednikov, Daniel , et. al "Experimental Setup for NOEMS". BGU faculty of EE , engineering project (2023).

## **10.Appendices:**

Laser beam entry:

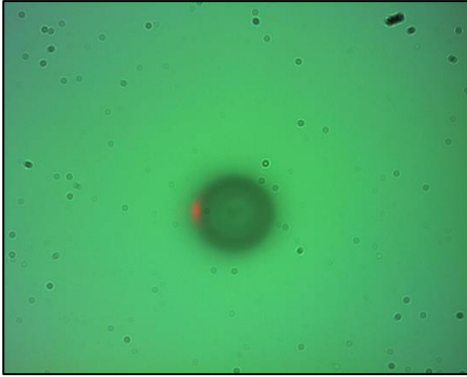


Figure 10.1: Laser beam entry

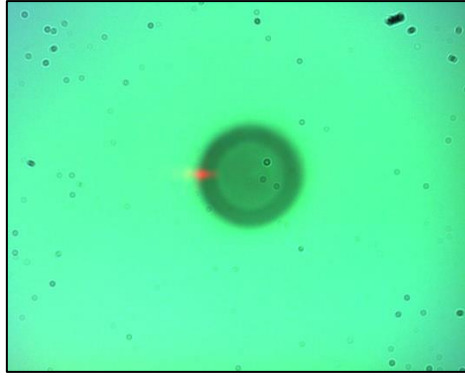


Figure 10.2: Laser beam entry

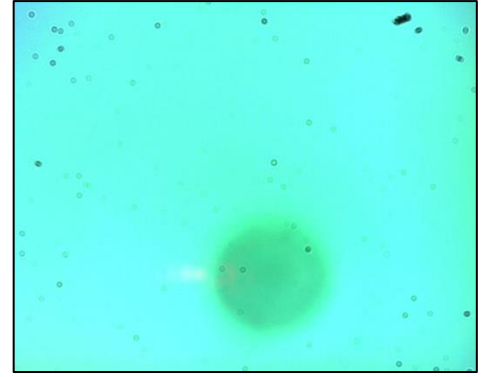


Figure 10.3: Laser beam entry

PNJ phenomena:

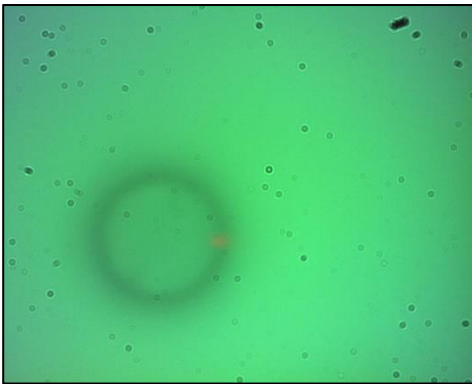


Figure 10.4: light exit

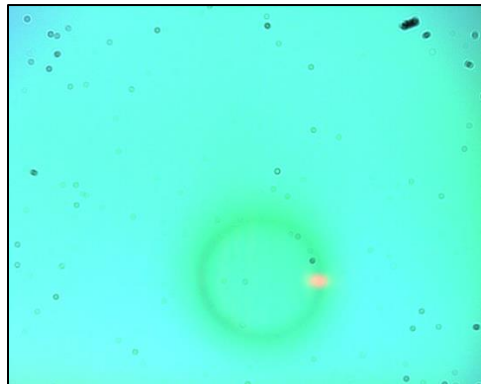


Figure 10.5: PNJ

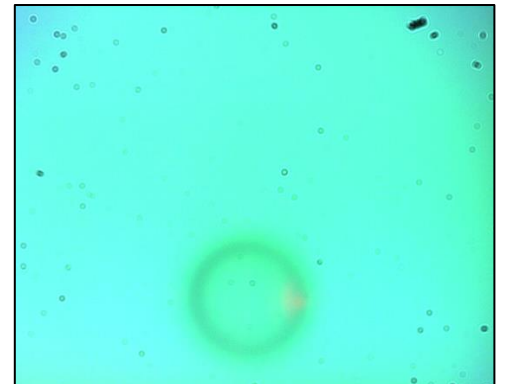


Figure 10.6: Small propagation

## המלצת ציון לדו"ח מסכם

אם יש צורך, לכל סטודנט/ית בנפרד

מספר הפרויקט: p-2024-051

שם הפרויקט: בניית מערך אופטי עבור מניפולציה ננו – אופטו – אלקטרו – מכאנית של ננו – חלקיקים

שם המנחה: פרופ' קרבצ'בסקי אלינה

שם הסטודנט: יעקב קוזמינסקי 206511966

אורן זברו 208118562

קריטריון	1-חלש	2-בינוני	3-טוב	4-ט"מ	5-מצוין
הגדרת המטרה - האם מטרת הפרויקט ברורה? המטרה צריכה לכלול גם את התרומה הצפויה מהשלמת הפרויקט.					
ארכיטקטורת הפתרון - האם הובהר מדוע הארכיטקטורה המוצעת לפתרון ההנדסי מתאימה לפתרון הבעיה? האם הייתה התייחסות לאלטרנטיבות?					
הצגת התוצאות - האם הוסברו המשמעויות של התוצאות, או המסקנות הנובעות מהן, האם רק הייתה הצגה עובדתית של תוצאות?					
מבנה – מצגת - האם יש מבנה הגיוני להצגת העבודה? מבוא, רקע ו-SoTA, מטרות, שיטה, פתרון, תוצאות, מסקנות.					
רמת קושי - כיצד הנך מעריך את הפרויקט בהשוואה לפרויקטים אחרים השנה או בשנים קודמות?					
איכות כתיבה / הצגה - נא להתייחס לאיכות הצגת העבודה: תחביר, מבנה וקשר הגיוני בין החלקים במהלך הצגת העבודה					
שורה תחתונה - האם מטרות הפרויקט הושגו? יש להתייחס למטרות כפי שהוגדרו בתחילה.					
הבנה - האם נראה שהסטודנט מבין את העבודה שנעשתה? האם עומק הדיון מספק?					

					השקעה - האם ניכר שהסטודנט השקיע בעבודה בפרויקט ו/או בהכנת ההצגה של העבודה? האם נראה שהעבודה נעשתה בחופזה, כדי לצאת ידי חובה?
					דירוג - כיצד הנך מעריך את איכות הפרויקט ביחס לכלל הפרויקטים שראית?
					המאפיינים העיקריים בפרויקט - יש לסמן את כמות המאפיינים שהושגו (ולו באופן חלקי). מאפיין אחד בעמודה 1 וכן הלאה... המאפיינים: * מימוש/יצור מערכת, * אנליזה מתמטית, * תכנון אלגוריתמי, * אינטגרציה עם מערכת קיימת, * חקר ביצועים . בקביעת הציון: העדר מאפיינים מזכה בציון 1, מאפיין אחד בלבד מזכה בציון 3, ושני מאפיינים ומעלה מזכים בציון 5.

אם יש כוונה לפרסם/ יפורסם מאמר, שם כתב העת ומועד משוער להגשה:

ציין אם יש כוונה לשקול המלצה כפרויקט מצטיין:

הערות נוספות: